

ARTICLE

Received 13 Jan 2016 | Accepted 1 Feb 2016 | Published 29 Mar 2016

DOI: 10.1038/ncomms10903

OPEN

Interplanar coupling-dependent magnetoresistivity in high-purity layered metals

N. Kikugawa^{1,2}, P. Goswami^{2,3}, A. Kiswandhi^{2,†}, E.S. Choi², D. Graf², R.E. Baumbach², J.S. Brooks², K. Sugii^{1,†}, Y. Iida¹, M. Nishio⁴, S. Uji¹, T. Terashima¹, P.M.C. Rourke^{5,†}, N.E. Hussey^{6,7}, H. Takatsu^{8,9,†}, S. Yonezawa⁹, Y. Maeno⁹ & L. Balicas²

The magnetic field-induced changes in the conductivity of metals are the subject of intense interest, both for revealing new phenomena and as a valuable tool for determining their Fermi surface. Here we report a hitherto unobserved magnetoresistive effect in ultra-clean layered metals, namely a negative longitudinal magnetoresistance that is capable of overcoming their very pronounced orbital one. This effect is correlated with the interlayer coupling disappearing for fields applied along the so-called Yamaji angles where the interlayer coupling vanishes. Therefore, it is intrinsically associated with the Fermi points in the field-induced quasi-one-dimensional electronic dispersion, implying that it results from the axial anomaly among these Fermi points. In its original formulation, the anomaly is predicted to violate separate number conservation laws for left- and right-handed chiral (for example, Weyl) fermions. Its observation in PdCoO₂, PtCoO₂ and Sr₂RuO₄ suggests that the anomaly affects the transport of clean conductors, in particular near the quantum limit.

¹National Institute for Materials Science, Tsukuba, Ibaraki 305-0003, Japan. ²Condensed Matter Group, National High Magnetic Field Laboratory, Florida State University, 1800 East Paul Dirac Drive, Tallahassee, Florida 32310, USA. ³Condensed Matter Theory Center, University of Maryland, College Park, Maryland 20742-4111, USA. ⁴National Institute for Materials Science, Tsukuba, Ibaraki 305-0047, Japan. ⁵H.H. Wills Physics Laboratory, University of Bristol, Tyndall Avenue, Bristol BS8 1TL, UK. ⁶High Field Magnet Laboratory (HFML-EMFL), Radboud University, Toernooiveld 7, 6525 ED Nijmegen, Nijmegen, The Netherlands. ⁷Institute of Molecules and Materials, Radboud University, Heyendaalseweg 135, 6525 AJ Nijmegen, The Netherlands. ⁸Department of Physics, Tokyo Metropolitan University, Tokyo 192-0397, Japan. ⁹Department of Physics, Graduate School of Science, Kyoto University, Kyoto 606-8502, Japan. † Present addresses: Department of Physics, University of Texas at Dallas, Richardson 75080, USA (A.K.); Institute for Solid State Physics, University of Tokyo, Kashiwa, Chiba 277-8581, Japan (K.S.); Department of Energy and Hydrocarbon Chemistry, Graduate School of Engineering, Kyoto University, Kyoto 615-8510, Japan (H. T.); National Research Council, Ottawa, Ontario, Canada K1A 0R6 (P.M.C.R.). Correspondence and requests for materials should be addressed to L.B. (email: balicas@magnet.fsu.edu).

The magnetoconductivity or -resistivity of metals under a uniform magnetic field $\mu_0 H$ (μ_0 is the permeability of free space) is highly dependent on the precise shape of their Fermi surface (FS) and on the orientation of the current flow relative to the external applied field $H^{1,2}$. This is particularly true for high-purity metals at low temperatures, whose carriers may execute many cyclotron orbits in between scattering events. However, the description of the magnetoconductivity of real systems in terms of the Boltzmann equation including the Lorentz force, the electronic dispersion and realistic scattering potentials is an incredibly daunting task, whose approximate solutions can only be obtained through over simplifications. Despite the inherent difficulty in describing the magneto-resistivity of metallic or semi-metallic systems, it continues to be a subject of intense interest. Indeed, in recent years, a number of new magnetoresistance phenomena have been uncovered. For example, although semi-classical transport theory predicts a magnetoresistivity $\rho(\mu_0 H) \propto (\mu_0 H)^2$, certain compounds such as β -Ag₂Te display a linear, non-saturating magnetoresistivity³, which is ascribed to the quantum magnetoresistive scenario⁴, associated with linearly dispersing Dirac-like bands⁵. However, in semi-metals characterized by a bulk Dirac dispersion and extremely high electron mobilities such as Cd₃As₂, the linear magnetoresistivity develops a weak $(\mu_0 H)^2$ term as the quality of the sample increases⁶. Its enormous magnetoresistivity is claimed to result from the suppression of a certain protection against backscattering channels⁶. The semi-metal WTe₂ was also found to display a very large and non-saturating magnetoresistivity, which is $\propto (\mu_0 H)^2$ under fields up to 60 T. This behaviour was ascribed to a nearly perfect compensation between the densities of electrons and holes⁷. In recent times, a series of compounds were proposed to be candidate Weyl semi-metals characterized by a linear touching between the valence and the conduction bands at several points (Weyl points) of their Brillouin zone⁸. These Weyl points are predicted to lead to a pronounced negative magnetoresistivity for electric fields aligned along a magnetic field due to the so-called axial anomaly^{9,10}.

Here we unveil the observation of yet another magnetoresistive effect, namely a pronounced negative magnetoresistivity in extremely clean and non-magnetic layered metals. We study the delafossite-type PtCoO₂ and PdCoO₂ compounds, which are characterized by a single FS sheet and, as with Cd₃As₂, can display residual resistivities on the order of a just few tenths of nΩ cm. Given its extremely low level of disorder, for specific field orientations along which the interlayer coupling vanishes, PdCoO₂ can display a very pronounced positive magnetoresistivity that exceeds 550,000% for $\mu_0 H \simeq 35$ T and for currents along the interlayer axis. Nevertheless, as soon as the field is rotated away from these specific orientations and as the field increases, this large orbital effect is overwhelmed by the emergence of a pronounced negative magnetoresistivity. For fields along the interlayer direction, a strong longitudinal negative magnetoresistivity is observed from $\mu_0 H = 0$ T to fields all the way up to $\mu_0 H = 35$ T. Very similar behaviour is observed in the PtCoO₂ compound. For the correlated Sr₂RuO₄, the longitudinal negative magnetoresistivity effect is also observable but only in the cleanest samples, that is, those displaying the highest superconducting transition temperatures. We suggest that this effect might result from the axial anomaly between Fermi points in a field-induced, quasi-one-dimensional electronic dispersion.

Results

Observation of an anomalous longitudinal magnetoresistivity.

As shown in Fig. 1a, PdCoO₂ crystallizes in the space group $R\bar{3}m(D_{3d}^5)$, which results from the stacking of monatomic

triangular layers¹¹. The synthesis of PdCoO₂ single crystals is described in the Methods section. According to band structure calculations^{12–14}, the Fermi level E_F is placed between the filled t_{2g} and the empty e_g levels with the Pd triangular planes dominating the conductivity and leading to its highly anisotropic transport properties. The reported room temperature in-plane resistivity is just 2.6 μΩ cm, making PdCoO₂ perhaps the most conductive oxide known to date¹⁵. Figure 1b,c show the configuration of contacts used for measuring the longitudinal magnetoresistivity of all compounds. de Haas van Alphen measurements¹⁵ reveal a single, corrugated and nearly two-dimensional FS with a rounded hexagonal cross-section, in broad agreement with both band structure calculations^{12–14} and angle-resolved photoemission measurements¹⁶. de Haas van Alphen yields an average Fermi wave vector $k_F = \sqrt{2eF/\hbar} = 9.5 \times 10^9 \text{ m}^{-1}$ or an average Fermi velocity $v_F = \hbar k_F / \mu = 7.6 \times 10^5 \text{ m s}^{-1}$ (where $\mu \simeq 1.5$ is the carrier effective mass¹⁵ in units of free electron mass). Recent measurements of interplanar magnetoresistivity $\rho_c(\mu_0 H)$ reveal an enormous enhancement for fields along the [110] direction, that is, increasing by $\sim 35,000\%$ at 2 K under $\mu_0 H = 14$ T, which does not follow the characteristic $\rho(\mu_0 H) \propto (\mu_0 H)^2$ dependence at higher fields¹⁷. This behaviour can be reproduced qualitatively by semi-classical calculations, assuming a very small scattering rate¹⁷. Most single crystals display in-plane residual resistivities ρ_{ab0} ranging from only ~ 10 up to ~ 40 nΩ cm, which correspond to transport lifetimes $\tau_{tr} = \mu / ne^2 \rho_{ab0}$ ranging from ≥ 20 down to $\simeq 5.5$ ps (e is the electron charge and $n \simeq 2.4 \times 10^{28} \text{ m}^{-3}$ (ref. 11)) or mean free paths $\ell = v_F \tau_{tr}$ ranging from ~ 4 up to 20 μm (ref. 15). However, according to ref. 15, the quasiparticle lifetime τ extracted from the Dingle temperature becomes (in units of length) $v_F \tau \sim 0.6$ μm. Hence, the transport lifetime is larger than the quasiparticle lifetime by at least one order of magnitude, which is the hallmark of a predominant forward scattering mechanism (see ref. 18). For a magnetic field along c axis, $\omega_c \tau_{tr} > 1$ when $\mu_0 H \geq 1$ T; in contrast, $\omega_c \tau > 1$ when $\mu_0 H > 10$ T. These estimations suggest the importance of the Landau quantization for understanding our observations over a wide range of fields up to $\mu_0 H \sim 30$ T.

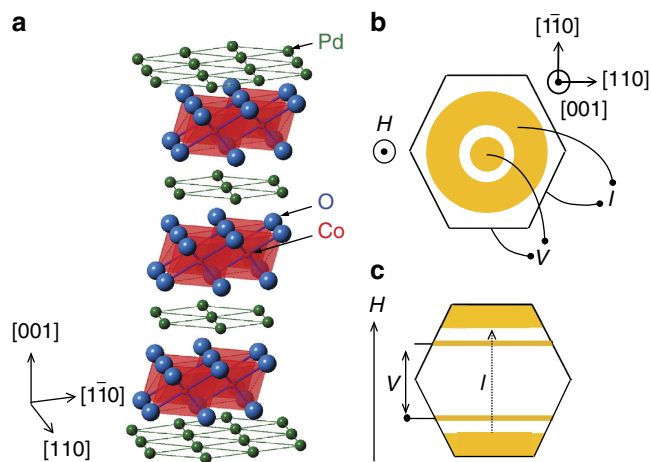


Figure 1 | Crystal structure of PdCoO₂ and configuration of electrical contacts. (a) Crystallographic structure of the delafossite PdCoO₂ with Pd, Co and O atoms shown in green, blue and red, respectively. (b) Configuration of contacts for measuring the interplanar longitudinal resistivity (ρ_c), showing concentric contacts at the top and at the bottom surface of each hexagonal platelet-like crystal. (c) Configuration of contacts for measuring the in-plane longitudinal resistivity ($\rho_{[1\bar{1}0]}$) for currents flowing along the $[1\bar{1}0]$ axis and fields applied along the same direction.

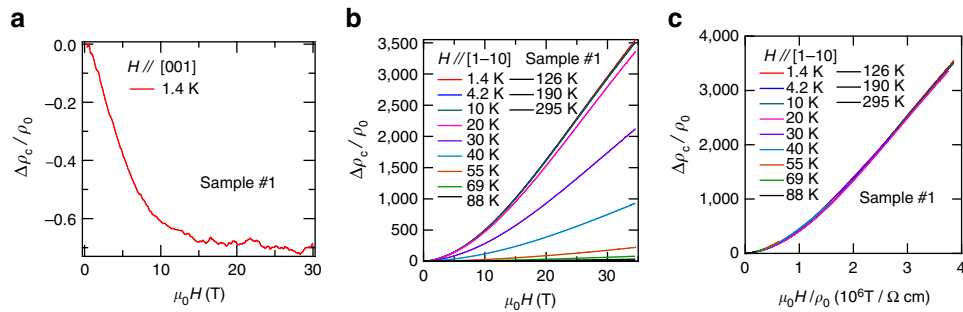


Figure 2 | Negative longitudinal and colossal orbital magnetoresistance of PdCoO₂. (a) Normalized interplanar magnetoresistivity $\Delta\rho_c/\rho_0 = (\rho_c(\mu_0H) - \rho_0)/\rho_0$, where ρ_0 is the resistivity at zero field, for a PdCoO₂ single crystal and as a function of $\mu_0H \parallel j$ axis at $T = 1.4$ K. The very pronounced negative longitudinal magnetoresistance arising in the presence of cyclotron motion in the ab plane is noteworthy. (b) $\Delta\rho_c(\mu_0H)/\rho_0$ as a function of μ_0H applied along the $[1\bar{1}0]$ direction and for several temperatures T , describing positive transverse magnetoresistance. At $T = 1.4$ K, $\Delta\rho_c$ surpasses 350,000% under a field $H = 35$ T. (c) Kohler scaling of the transverse positive magnetoresistance $\Delta\rho_c(\mu_0H)$. It is noteworthy that (i) all data collapse on a single curve as a function of μ_0H/ρ_0 and (ii) at low fields $\Delta\rho_c(\mu_0H)/\rho_0 \propto (\mu_0H/\rho_0)^2$ as expected for classical orbital magnetoresistance.

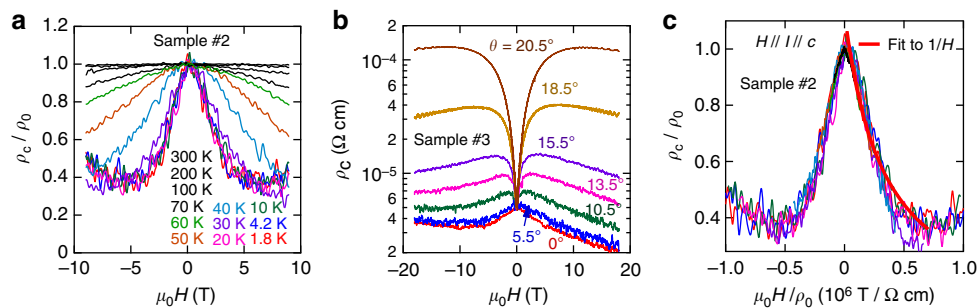


Figure 3 | Anomalous magnetoresistive response of PdCoO₂. (a) Interlayer resistivity ρ_c normalized by its zero-field value ρ_0 as a function of the external field μ_0H and for μ_0H parallel to current I (itself parallel to the sample interlayer c -axis) and for several temperatures T . It is noteworthy that the very pronounced negative magnetoresistivity, that is, ρ_c/ρ_0 decreases by a factor $> 60\%$ when sweeping the field from 0 to 5 T. It is also worth noting that this effect disappears when the T approaches and/or surpasses ~ 200 K. (b) ρ_c as a function of μ_0H from a third crystal at $T = 1.8$ K and for several angles θ between μ_0H and the c axis. It is noteworthy how the negative magnetoresistivity observed at low fields is progressively suppressed as θ increases, becoming strongly positive. Nevertheless, the mechanism leading to the negative magnetoresistivity is observed to overpower the orbital one at higher fields and higher angles. (c) Kohler plot for all the temperature-dependent ρ_c/ρ_0 . Red line is a fit of $\Delta\rho_c/\rho_0$ to $(\mu_0H)^{-1}$.

As shown in Fig. 2a, the low- T magnetoresistivity or $\Delta\rho_c = (\rho_c - \rho_0)/\rho_0$, where ρ_0 is the zero-field interplanar resistivity, decreases (up to $\sim 70\%$) in a magnetic field of 30 T oriented parallel to the applied current. Given that PdCoO₂ is non-magnetic and extremely clean (see Methods), this effect cannot be attributed to magnetic impurities. In addition, the magnitude of the observed magnetoresistivity cannot be explained in terms of weak localization effects^{19,20}. To support both statements, in Fig. 2b we show $\Delta\rho_c$ for a PdCoO₂ single crystal as a function of H applied along the $[1\bar{1}0]$ planar direction and for several temperatures T . In sharp contrast to results shown in Fig. 2a, as T decreases, $\Delta\rho_c(\mu_0H)$ increases considerably, by more than three orders of magnitude when $T < 10$ K, thus confirming the absence of scattering by magnetic impurities or any role for weak localization. In addition, it is noteworthy that $\Delta\rho_c \propto (\mu_0H)^2$ at low fields, which indicates that the interlayer transport is coherent at low fields²¹. Figure 2c depicts a simple Kohler plot of the magnetoresistivity shown in Fig. 2b, where the field has also been normalized by $\rho_0(T)$, which indicates unambiguously that the transverse magnetoresistive effect in PdCoO₂ is exclusively orbital in character and is dominated by the scattering from impurities/imperfections and phonons¹.

The evolution of the longitudinal magnetoresistance with temperature is depicted in Fig. 3a. ρ_c is seen to decrease by a factor surpassing 60% for fields approaching 9 T and for all temperatures below 30 K. Figure 3b displays $\rho_c(\mu_0H)/\rho_0$ as a

function of the angle θ between μ_0H and the c axis at a temperature $T = 1.8$ K, for a third single crystal. For $\theta > 10^\circ$, the pronounced positive magnetoresistance observed at low fields, due to an orbital magnetoresistive effect, is overpowered at higher fields by the mechanism responsible for the negative magnetoresistivity. This behaviour is no longer observed within this field range when θ is increased beyond $\sim 20^\circ$. Figure 3c shows a Kohler plot, that is, $\Delta\rho_c/\rho_0$ as a function of μ_0H normalized by ρ_0 . As seen in Fig. 3c, all curves collapse on a single curve, indicating that a particular transport mechanism dominates even at high temperatures where phonon scattering is expected to be strong. The red line is a fit to $(\mu_0H)^{-1}$, indicating that $\rho_c^{-1} = \sigma_c \propto \mu_0H$ at lower fields.

Angular dependence of the anomalous magnetoresistive response.

Fig. 4 shows the longitudinal magnetoresistance $\rho_{[1\bar{1}0]}(\mu_0H)/\rho_0$ for fields and currents along the $[1\bar{1}0]$ axis. For this orientation, the charge carriers follow open orbits along the axis of the cylindrical FS instead of quantized cyclotronic orbits. In contrast to $\Delta\rho_c/\rho_0$, but similar to the longitudinal magnetoresistivity of ultra-clean elemental metals^{1,2}, $\rho_{[1\bar{1}0]}(\mu_0H)/\rho_0$ is observed to increase and saturate as a function of μ_0H . This further confirms that conventional mechanisms, for example, impurities, magnetism and so on, are not responsible for the negative longitudinal magnetoresistivity observed in $\Delta\rho_c/\rho_0$.

Figure 5a shows ρ_c as a function of the angle θ between the field and the c axis, for three different field values: 8, 25 and 30 T. $\rho_c(\theta)$ displays the characteristic structure displayed by quasi-two-dimensional metals, namely a series of sharp peaks at

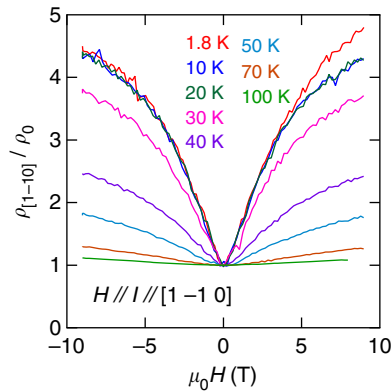


Figure 4 | Longitudinal magnetoresistance for fields along the planes. In-plane longitudinal resistivity $\rho_{[1\bar{1}0]}$ normalized by its zero field value ρ_0 as a function of the field applied along the $[1\bar{1}0]$ direction, for a PdCoO_2 single crystal and for several temperatures. The absence of negative magnetoresistivity is noteworthy.

specific angles $\theta_n = \arctan(\pi(n-1/4)/ck_F^{\parallel})$ called the Yamaji angles (where n is an integer, c is the interplanar distance and k_F^{\parallel} is the projection of the Fermi wave number on the conduction plane), for which all cyclotronic orbits on the FS have an identical orbital area²². In other words, the corrugation of the FS no longer leads to a distribution of cross-sectional areas, as if the corrugation has been effectively suppressed. As discussed below, in terms of the energy spectrum, this means that the Landau levels become non-dispersive at the Yamaji angles^{18,23}; hence, one no longer has Fermi points. The sharp peak at $\theta = 90^\circ$ is attributed to coherent electron transport along small closed orbits on the sides of a corrugated cylindrical FS^{24,25}. The width of this peak $\Delta\theta$, shown in Fig. 5b for several temperatures, allows us to estimate the interlayer transfer integral t_c (ref. 26),

$$\Delta\theta \approx \frac{2k_F^{\parallel}t_c d}{E_F} \rightarrow t_c \approx \frac{\Delta\theta E_F}{2k_F^{\parallel}d} \quad (1)$$

assuming a simple sinusoidal FS corrugation along the k_z direction. Here, the interplanar separation is $d = c/3$, as there are three conducting Pd planes per unit cell, each providing one conducting hole and therefore leading to three carriers per unit cell. This value is consistent with our Hall-effect measurements (not included here). The full width at half maximum of the peak at 90° is $\Delta\theta \approx 0.78^\circ$ and E_F is given by $\hbar^2 k_F^2 / 2\mu = 2.32$ eV; therefore, one obtains $t_c = 2.79$ meV or ≈ 32.4 K. Figure 5c displays ρ_c as a function of μ_0H for two angles; the Yamaji

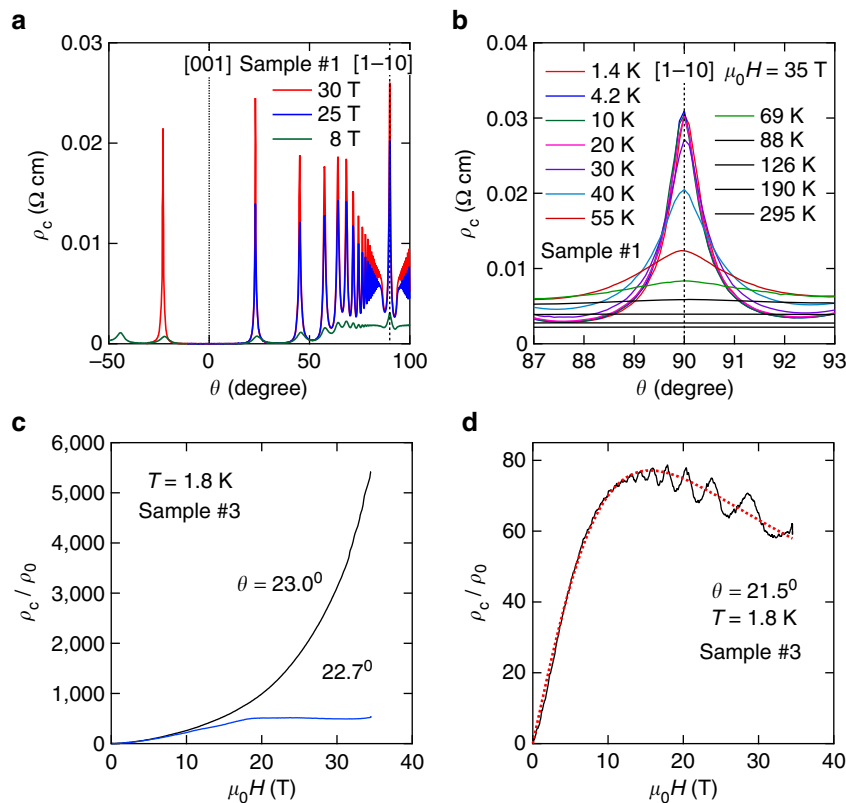


Figure 5 | Angular magnetoresistance oscillations for a PdCoO_2 single crystal. (a) Interplanar magnetoresistivity ρ_c for a PdCoO_2 single crystal as a function of the angle θ between the $[001]$ interplanar direction and the external field μ_0H . The pronounced peaks observed as a function of θ are the so-called Yamaji-effect peaks²². (b) Interlayer coherence peak observed for fields nearly along the interplanar direction, which indicates an extended FS along the interlayer direction²⁴. From the width $\Delta\theta$ of the peak at half maximum, one can estimate the value of the interlayer transfer integral $t_c = 2.79$ meV from equation (1). (c) Interplanar resistivity ρ_c as a function of μ_0H at $T = 1.8$ K and for two angles, that is, the Yamaji value $\theta_{n=1} = 23.0^\circ$ and $\theta = 22.7^\circ$. It is noteworthy how the pronounced positive magnetoresistivity observed at $\theta_{n=1}$ is strongly suppressed when μ_0H is rotated by just $\sim 0.3^\circ$, leading to magnetoresistance saturation. (d) ρ_c as a function of μ_0H under $T = 1.8$ K and for $\theta = 21.5^\circ$. It is noteworthy how ρ_c , after increasing by several orders of magnitude, displays negative magnetoresistivity at higher fields, thus indicating a clear competition between the orbital and another mechanism, which suppresses the magnetoresistivity. Dotted red line corresponds to a fit of $\rho_c = 1/\sigma_c^{-1} = (\sigma_0 + \alpha\mu_0H + \beta/\mu_0H)^{-1}$.

angle $\theta_{n=1} = 23.0^\circ$ and $\theta = 22.7^\circ$, respectively. As seen, $\rho_c(\mu_0H)$ for fields along $\theta_{n=1}$ displays a very pronounced positive magnetoresistance, that is, ρ_c/ρ_0 increases by $\sim 550,000\%$ when μ_0H is swept from 0 to 35 T. However, at $\mu_0H = 35$ T, ρ_c/ρ_0 decreases by one order of magnitude as μ_0H is rotated by just $\sim 0.3^\circ$ with respect to $\theta_{n=1}$. Furthermore, as seen in Fig. 5d, at higher fields ρ_c displays a cross-over from a very pronounced and positive to a negative magnetoresistance, resulting from a small increment in θ relative to $\theta_{n=1}$. This is a very clear indication for two competing mechanisms, with negative magnetoresistivity overcoming the orbital effect when the orbitally averaged interlayer group velocity (or the transfer integral t_c) becomes finite at $\theta \neq \theta_n$. We emphasize that for a conventional and very clean metal, composed of a single FS sheet, the magnetoresistivity should either be $\propto (\mu_0H)^2$ (ref. 21) or saturate as seen in quasi-two-dimensional metals close to the Yamaji angle²⁷, or in Fig. 2a,b for fields below ~ 15 T. This is illustrated by the Supplementary Fig. 1 (see also Supplementary Note 1), which contrasts our experimental observations with predictions based on semi-classical transport models, which correctly describe the magnetoresistance of layered organic metals in the vicinity of the Yamaji angle. In contrast, as illustrated by the dotted red line in Fig. 5d, $\rho_c(\mu_0H)$ can be well described by the expression $\rho_c(\mu_0H) = \sigma_c^{-1} = (\sigma_0 + \alpha\mu_0H + \beta/\mu_0H)^{-1}$. Here, the $\rho_c \propto (\mu_0H)^{-1}$ term describes the negative magnetoresistivity as previously seen in Fig. 3, whereas the $\rho_c \propto \mu_0H$ term describes the non-saturating linear magnetoresistance predicted and observed for systems close to the quantum limit^{3–5,28}. This expression describes $\rho_c(\mu_0H, \theta)$ satisfactorily, except at the Yamaji angle where both terms vanish. In the neighbourhood of θ_n , the addition of a small $\rho_c \propto (\mu_0H)^2$ term improves the fit, with its pre-factor increasing as θ_n is approached. ρ_c also displays Shubnikov de Haas oscillations at small (and strongly θ dependent) frequencies, which were not previously detected in ref. 15. As discussed in ref. 29, these slow oscillations, observed only in the interlayer magnetoresistance of layered metals, originate from the warping of the FS. In Supplementary Fig. 2 (See also Supplementary Note 2), we show how these frequencies disappear when the group velocity vanishes at θ_n .

Significantly, this effect does not appear to be confined to PdCoO₂. Figure 6 presents an overall evaluation of the longitudinal magnetoresistance of isostructural PtCoO₂, whereas Supplementary Fig. 3 displays the observation of impurity-dependent negative magnetoresistivity in the correlated

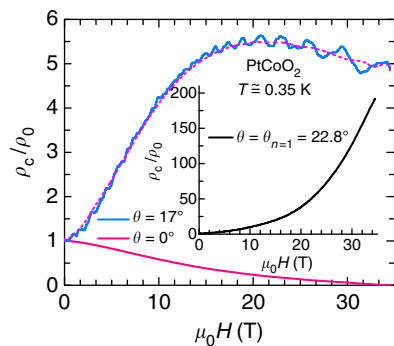


Figure 6 | Negative longitudinal magnetoresistance in PtCoO₂.

Interplanar resistivity ρ_c normalized by its zero-field value ρ_0 for a PtCoO₂ single crystal at a temperature $T = 0.35$ K and as a function of the magnetic field μ_0H applied along two angles with respect to the c axis, respectively $\theta = 0^\circ$ (pink line) and 17° (blue line). Dashed magenta line describes the smoothly varying background. Inset: ρ_c/ρ_0 as a function of μ_0H applied along the first Yamaji angle $\theta_n = 22.8^\circ$.

perovskite Sr₂RuO₄ (See also Supplementary Note 3). As shown in Fig. 6, PtCoO₂ presents a pronounced negative longitudinal magnetoresistivity either for $\mathbf{j} \parallel \mathbf{H} \parallel c$ axis or for μ_0H close to an Yamaji angle (\mathbf{j} is the current density). It also presents a very pronounced and non-saturating magnetoresistivity for fields applied along the Yamaji angle. For both systems, the magnetoresistivity does not follow a single power law as a function of μ_0H . In fact, as shown in Supplementary Fig. 4, at θ_n the magnetoresistivity of the (Pt,Pd)CoO₂ system follows a $(\mu_0H)^2$ dependence for $\mu_0H \lesssim 15$ T. At intermediate fields, $\rho(\mu_0H)$ deviates from the quadratic dependence, recovering it again at subsequently higher fields. As Kohler's rule implies that $\Delta\rho/\rho_0 \propto (\mu_0H/\rho_0)^2$, we argue that the observed increase in slope would imply a field-dependent reduction in scattering by impurities (see Supplementary Fig. 4 and Supplementary Note 4). The precise origin of this suppression in scattering remains to be identified. Nevertheless, the enormous and positive magnetoresistivity observed for fields along θ_n seems consistent with a simple scenario, that is, an extremely clean system(s) whose impurity scattering weakens with increasing magnetic field. In Sr₂RuO₄, the negative longitudinal magnetoresistivity is observed only in the cleanest samples and for angles within 10° away from the c axis. This compound is characterized by three corrugated cylindrical FS sheets, each leading to a distinct set of Yamaji angles, making it impossible to completely suppress the interplanar coupling at specific Yamaji angle(s).

Discussion

Negative magnetoresistivity is a common feature of ferromagnetic metals near their Curie temperature, or of samples having dimensions comparable to their electronic mean free path where the winding of the electronic orbits under a magnetic field reduces the scattering from the surface. It can also result from the field-induced suppression of weak localization or from the field-induced suppression of spin-scattering/quantum-fluctuations as seen in f -electron compounds³⁰. None of the compounds described in this study are near a magnetic instability, nor do they contain significant amounts of magnetic impurities or disorder to make them prone to weak localization. The magnitude of this anomalous magnetoresistivity, coupled to its peculiar angular dependence, are in fact enough evidence against any of these conventional mechanisms. Below, we discuss an alternative scenario based on the axial anomaly, which in our opinion explains most of our observations.

The axial anomaly is a fundamental concept of relativistic quantum field theory, which describes the violation of separate number conservation laws of left- and right-handed massless chiral fermions in odd spatial dimensions due to quantum mechanical effects^{31,32}. When three-dimensional massless Dirac or Weyl fermions are placed under parallel electric and magnetic fields, the number difference between the left and the right-handed fermions is expected to vary with time according to the Adler–Bell–Jackiw formula^{9,33}

$$\partial_t(n_R - n_L) = \frac{e^2 EB}{2\pi^2 \hbar^2}. \quad (2)$$

Here, $n_{R/L}$ are the number operators for the right- and the left-handed Weyl fermions, with the electric and the magnetic field strengths respectively given by E and B . The Dirac fermion describes the linear touching of twofold Kramer's degenerate conduction and valence bands at isolated momentum points in the Brillouin zone. By contrast, the Weyl fermions arise due to the linear touching between nondegenerate conduction and valence bands. The axial anomaly was initially proposed to produce a large, negative longitudinal magnetoresistance, for a class of gapless semiconductors, for which the low-energy band structure

is described by massless Weyl fermions¹⁰. The reason for the negative magnetoresistance is relatively straightforward. The number imbalance due to axial anomaly can only be equilibrated through backscattering between two Weyl points. This involves a large momentum transfer \mathbf{Q}_W . Quite generally the impurity scattering in a material can be modeled by a momentum dependent impurity potential $V(\mathbf{Q})$, where \mathbf{Q} is the momentum transfer between the initial and the final electronic states. If $V(\mathbf{Q})$ is a smoothly decreasing function of $|\mathbf{Q}|$ (such as Gaussian or Lorentzian), the backscattering amplitude can be considerably smaller than its forward scattering counterparts (occurring with small \mathbf{Q} around each Weyl point). Therefore in the presence of axial anomaly the transport lifetime can be considerably larger than the one in the absence of a magnetic field. Consequently the axial anomaly in the presence of parallel \mathbf{E} and \mathbf{B} fields can give rise to larger conductivity or smaller resistivity i.e., negative magnetoresistance. Recent theoretical proposals for Weyl semi-metals^{34–37} followed by experimental confirmation^{38,39} have revived the interest in the experimental confirmation of the axial anomaly through efforts in detecting negative longitudinal magnetoresistivity^{40–46}. There are examples of three-dimensional Dirac semi-metals^{47–49}, which may be converted, through Zeeman splitting, into a Weyl semi-metal. Examples include $\text{Bi}_{1-x}\text{Sb}_x$ at the band inversion transition point between topologically trivial and nontrivial insulators⁴², and Cd_3As_2 (ref. 6).

In analogy with the predictions for the axial anomaly between Weyl points, here we suggest that our observations might be consistent with the emergence of the axial anomaly among the Fermi points of a field-induced, one-dimensional electronic dispersion¹⁸. In effect, in the presence of a strong magnetic field, the quantization of cyclotron motion leads to discrete Landau levels with one-dimensional dispersion and a degeneracy factor eB/h , see Fig. 7a–c. Consider the low-energy description of a one-dimensional electron gas, in terms of the right- and left-handed fermions obtained in the vicinity of the two Fermi points. In the presence of an external electric field E , the separate number conservation of these chiral fermions is violated according to

$$\partial_t(n_R - n_L) = \frac{eE}{\pi\hbar}, \quad (3)$$

where $n_{R/L}$ corresponds to the number operators of the right- and left-handed fermions, respectively^{31,32}. Each partially occupied Landau level leads to a set of Fermi points and the axial anomaly for such a level can be obtained from equation 3, after multiplying by eB/h . Therefore, each level has an axial anomaly determined by equation (2). When only one Landau level is partially filled, we have the remarkable universal result for the axial anomaly described by Adler–Bell–Jackiw formula of equation (2). For a non-relativistic electron gas, this would occur at the quantum limit. In contrast, this situation would naturally occur for Dirac/Weyl semi-metals, when the Fermi level lies at zero energy, that is, the material has a zero carrier density. Figure 7b describes the situation for a quasi-two-dimensional electronic system on approaching the quantum limit, or when the interplanar coupling becomes considerably smaller than the inter Landau level separation (for example, in the vicinity of the Yamaji angle). We emphasize that the observation of a pronounced, linear-in-field magnetoresistive component, as indicated by the fit in Fig. 5d, is a strong experimental evidence for the proximity of PdCoO_2 to the quantum limit on approaching the Yamaji angle. Therefore, we conclude that the axial anomaly should be present in every three-dimensional conducting system, on approaching the quantum limit. Explicit calculations indicate that the axial anomaly would only cause negative magnetoresistance for predominant forward scattering

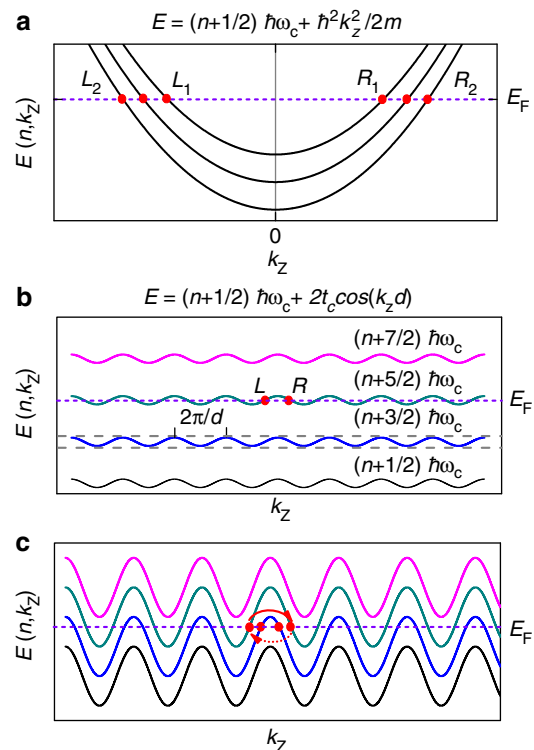


Figure 7 | Field-induced electronic dispersion for metals of different dimensionality.

(a) The dispersion of Landau levels for a conventional three-dimensional metal placed in an external magnetic field applied along the z -direction. Owing to the underlying parabolic dispersion, each Landau level disperses quadratically as a function of k_z , the momentum component along the applied field. Each partially occupied Landau level intersects the Fermi energy E_F at two Fermi points, as indicated by the red dots. In the vicinity of the two Fermi points located at $k_z = \pm k_{F,n}$ for the n -th partially filled Landau level, the quasiparticles disperse linearly with opposite group velocities $v_{\pm,n} = \pm \hbar k_{F,n} / \mu$ where μ is the effective mass. The \pm signs of the group velocity respectively define the chirality of the right- and the left-moving one-dimensional fermions. (b) In contrast, for quasi-two-dimensional metals the Landau levels possess a periodic dispersion relation as a function of k_z , owing to the tight binding term $2t_c \cos(k_z d)$, with interlayer hopping strength and spacing, respectively, given by t_c and d . Within the first Brillouin zone defined as $-\pi/d < k_z < \pi/d$, each partially filled Landau level again gives rise to a pair of one-dimensional fermions of opposite chirality around the Fermi points. The situation depicted here corresponds to $4t_c < \hbar\omega_c$, or when only one Landau level is partially filled. (c) Landau levels for $4t_c > \hbar\omega_c$ or when multiple Landau levels are partially occupied and each of them gives rise to a pair of chiral fermions.

produced by ionic impurities^{18,50}. $\rho(\mu_0 H) \propto (\mu_0 H)^{-1}$ as observed here (Figs 3 and 5) would result from Gaussian impurities¹⁸. As our experimental results show, PdCoO_2 is a metal of extremely high conductivity, thus necessarily dominated by small-angle scattering processes and therefore satisfying the forward scattering criterion. In this metal the Landau levels disperse periodically as shown in Fig. 7b,c, depending on the relative strength of the cyclotron energy $\hbar\omega_c = \hbar eB/\mu$ with respect to the interlayer transfer integral t_c . The condition $4t_c > \hbar\omega_c$ is satisfied when $\mu_0 H$ roughly exceeds 100 T. For this reason, Fig. 7c, with multiple partially occupied Landau levels, describes PdCoO_2 for fields along the c axis or for arbitrary angles away from the Yamaji ones. Nevertheless, one can suppress the Fermi points by aligning the field along an Yamaji angle and this should suppress the associated axial anomaly. As experimentally seen, the suppression of the Fermi points suppresses the

negative magnetoresistivity, indicating that the axial anomaly is responsible for it.

In summary, in very clean layered metals we have uncovered a very clear correlation between the existence of Fermi points in a one-dimensional dispersion and the observation of an anomalous negative magnetoresistivity. The suppression of these points leads to the disappearance of this effect. This indicates that the axial anomaly and related negative magnetoresistivity would not be contingent on the existence of an underlying three-dimensional Dirac/Weyl dispersion. Instead, our study in PdCoO₂, PtCoO₂ and Sr₂RuO₄, which are clean metals with no Dirac/Weyl dispersion at zero magnetic field, indicates that the axial anomaly and its effects could be a generic feature of metal(s) near the quantum limit. Nevertheless, the detection of negative magnetoresistivity would depend on the underlying scattering mechanisms, that is, observable only in those compounds that are clean enough to be dominated by elastic forward scattering^{18,50}. In a generic metal with a high carrier density, it is currently impossible to reach the quantum limit; for the available field strength, many Landau levels would be populated, thus producing a myriad of Fermi points. In this regard, extremely pure layered metals such as (Pd,Pt)CoO₂ are unique, as by just tilting the magnetic field in the vicinity of the Yamaji angle one can achieve the condition of a single, partially filled Landau level as it would happen at the quantum limit. An explicit analytical calculation of transport lifetime in the presence of axial anomaly due to multiple partially filled Landau levels is a technically challenging task. Therefore at present we do not have a simple analytical formula for describing the observed $(\mu_0 H)^{-1}$ behavior of the negative magnetoresistance along the *c* axis (for magnetic field strengths much smaller than the one required to reach the quantum limit). Nevertheless, the suppression of this negative magnetoresistivity for fields precisely aligned along the Yamaji angles indicates unambiguously that the electronic structure at the Fermi level is at the basis for its underlying mechanism. The observation of $(\mu_0 H)^{-1}$ behavior in the magnetoresistance around the Yamaji angle (when only one partially filled Landau level contributes) gives us the valuable insight that the anomaly induced negative magnetoresistance is quite robust irrespective of the number of partially filled Landau levels. However the determination of a precise functional form for the magnetoresistance in the presence of multiple partially filled Landau levels remains as a technical challenge for theorists. The situation is somewhat analogous to that of the Weyl semi-metals, which are characterized by a number of Weyl points in the first Brillouin zone³⁷, and apparently with all Weyl points contributing to its negative longitudinal magnetoresistivity⁴⁶. Hence, our results suggest that the axial anomaly among pairs of chiral Fermi points may play a role in ultra-clean systems even when they are located far from the quantum limit.

Finally, it is noteworthy that negative longitudinal magnetoresistivity is also seen in kish graphite at high fields, which is characterized by ellipsoidal electron- and hole-like FSs, on approaching the quantum limit and before the onset of a many-body instability towards a field-induced insulating density-wave ground state⁵¹. As discussed in ref. 18, the axial anomaly on approaching the quantum limit may also play a role for the negative magnetoresistivities observed in ZrTe₅ (ref. 52) and in $\alpha - (\text{ET})_2\text{I}_3$ (ref. 53), indicating that this concept, which is the basis of our work, is likely to be relevant to a number of physical systems, in particular semi-metals.

Methods

Crystal synthesis. Single crystals of PdCoO₂ were grown by the self-flux method through the following reaction PdCl₂ + 2CoO → PdCoO₂ + CoCl₂ with starting powders of PdCl₂ (99.999%) and CoO (99.99 + %). These powders were ground for up to 60 min and placed in a quartz tube. The tube was sealed in vacuum and

heated up to 930 °C in a horizontal furnace within 2 h and subsequently up to 1,000 °C within 6 h, and then cooled down quickly to 580 °C in 1 or 2 h. The tube is heated up again to 700 °C within 2 h, kept at 700 °C for 40 h and then cooled down to room temperature at 40 °C h⁻¹. Single crystals, with sizes of approximately 2.8 × 1.3 × 0.3 mm³ were extracted by dissolving out CoCl₂ with hot ethanol.

Single-crystal characterization. These were characterized by powder X-ray diffraction, energy dispersive X-ray analysis and electron probe microanalysis. The powder X-ray diffraction pattern indicated no impurity phases. In the crystals measured for this study, electron probe microanalysis indicated that the ratio of Pd to Co is 0.98:1, and that the amount of Cl impurities is <200 p.p.m.

Experimental setup. Transport measurements were performed by using conventional four-terminal techniques in conjunction with a Physical Properties Measurement System, a 18-T superconducting solenoid and a 35-T resistive magnet, coupled to cryogenic facilities such as ³He systems and variable temperature inserts.

References

- Pippard, A. B. *Magnetoresistance in Metals: Cambridge Studies in Low Temperature Physics 2* (Cambridge Univ. Press, 1989).
- Pippard, A. B. Longitudinal magnetoresistance. *Proc. R. Soc. A* **A282**, 464–484 (1964).
- Lee, M., Rosenbaum, T. F., Saboungi, M. L. & Schnyders, H. S. Band-gap tuning and linear magnetoresistance in the silver chalcogenides. *Phys. Rev. Lett.* **88**, 066602 (2002).
- Abrikosov, A. A. Quantum linear magnetoresistance. *Europhys. Lett.* **49**, 789793 (2000).
- Zhang, W. *et al.* Topological aspect and quantum magnetoresistance of β -Ag₂Te. *Phys. Rev. Lett.* **106**, 156808 (2011).
- Liang, T. *et al.* Ultrahigh mobility and giant magnetoresistance in the Dirac semi-metal Cd₃As₂. *Nat. Mater.* **14**, 280–284 (2015).
- Ali, M. N. *et al.* Large, non-saturating magnetoresistance in WTe₂. *Nature* **514**, 205–208 (2014).
- Huang, S.-M. *et al.* Theoretical discovery/prediction: Weyl semimetal states in the TaAs material (TaAs, NbAs, NBP, TaP) class. *Nat. Commun.* **6**, 7373 (2015).
- Bell, J. S. & Jackiw, R. A PCAC puzzle: $\pi_0 \rightarrow \gamma\gamma$ in the σ -model. *Nuovo Cimento A* **60**, 47–61 (1969).
- Nielsen, H. B. & Ninomiya, M. The Adler-Bell-Jackiw anomaly and weyl fermions in a crystal. *Phys. Lett. B* **130B**, 389–396 (1983).
- Takatsu, H. *et al.* Roles of high-frequency optical phonons in the physical properties of the conductive delafossite PdCoO₂. *J. Phys. Soc. Jpn* **76**, 104701 (2007).
- Eyert, V., Frésard, R. & Maignan, A. On the metallic conductivity of the delafossites PdCoO₂ and PtCoO₂. *Chem. Mater.* **20**, 2370–2373 (2008).
- Seshadri, R., Felser, C., Thieme, K. & Tremel, W. Metal-metal bonding and metallic behavior in some ABO₂ delafossites. *Chem. Mater.* **10**, 2189–2196 (1998).
- Kim, K., Choi, H. C. & Min, B. I. Fermi surface and surface electronic structure of delafossite PdCoO₂. *Phys. Rev. B* **80**, 035116 (2009).
- Hicks, C. W. *et al.* Quantum oscillations and high carrier mobility in the delafossite PdCoO₂. *Phys. Rev. Lett.* **109**, 11640 (2012).
- Noh, H. J. *et al.* Anisotropic electric conductivity of delafossite PdCoO₂ studied by angle-resolved photoemission spectroscopy. *Phys. Rev. Lett.* **102**, 256404 (2009).
- Takatsu, H. *et al.* Extremely large magnetoresistance in the nonmagnetic metal PdCoO₂. *Phys. Rev. Lett.* **111**, 056601 (2013).
- Goswami, P., Pixley, J. & Das Sarma, S. Axial anomaly and longitudinal magnetoresistance of a generic three dimensional metal. *Phys. Rev. B* **92**, 075205 (2015).
- Hikami, S., Larkin, A. I. & Nagaoka, Y. Spin-orbit interaction and magnetoresistance in the two-dimensional random system. *Prog. Theor. Phys.* **63**, 707–710 (1980).
- Bergmann, G. Weak localization in thin films a time-of-flight experiment with conduction electrons. *Phys. Rep.* **107**, 1–58 (1984).
- Moses, P. & Mackenzie, R. H. Comparison of coherent and weakly incoherent transport models for the interlayer magnetoresistance of layered Fermi liquids. *Phys. Rev. B* **60**, 7998 (1999).
- Yamaji, K. On the angle dependence of the magnetoresistance in quasi-two-dimensional organic superconductors. *J. Phys. Soc. Jpn* **58**, 1520–1523 (1989).
- Kurihara, Y. A microscopic calculation of the angular-dependent oscillatory magnetoresistance in quasi-two-dimensional systems. *J. Phys. Soc. Jpn* **61**, 975–982 (1992).

24. Singleton, J. *et al.* Test for interlayer coherence in a quasi-two-dimensional superconductor. *Phys. Rev. Lett.* **88**, 037001 (2002).
25. Hanasaki, H., Kagoshima, S., Hasegawa, T., Osada, T. & Miura, N. Contribution of small closed orbits to magnetoresistance in quasi-two-dimensional conductors. *Phys. Rev. B* **57**, 1336–1339 (1998).
26. Uji, S. *et al.* Fermi surface and angular-dependent magnetoresistance in the organic conductor (BEDT-TTF)₂Br(DIA). *Phys. Rev. B* **68**, 064420 (2003).
27. Yagi, R., Iye, Y., Osada, T. & Kagoshima, S. Semiclassical interpretation of the angular-dependent oscillatory magnetoresistance in quasi-two-dimensional systems. *J. Phys. Soc. Jpn* **59**, 3069–3072 (1990).
28. Hu, J. & Rosenbaum, T. F. Classical and quantum routes to linear magnetoresistance. *Nat. Mater.* **7**, 697–700 (2008).
29. Kartsovnik, M. V., Grigoriev, P. D., Biberacher, W., Kushch, N. D. & Wyder, P. Slow oscillations of magnetoresistance in quasi-two-dimensional metals. *Phys. Rev. Lett.* **89**, 126802 (2002).
30. Zeng, B. *et al.* CeCu₂Ge₂: challenging our understanding of quantum criticality. *Phys. Rev. B* **90**, 155101 (2014).
31. Peskin, M. E. & Schroeder, D. V. *An Introduction to Quantum Field Theory* (Addison-Wesley, 1995).
32. Fujikawa, K. & Suzuki, H. *Path Integrals and Quantum Anomalies* (Clarendon Press, 2004).
33. Adler, S. Axial-vector vertex in spinor electrodynamics. *Phys. Rev.* **177**, 2426–2438 (1969).
34. Wan, X., Turner, A., Vishwanath, A. & Savrasov, S. Y. Topological semimetal and Fermi-arc surface states in the electronic structure of pyrochlore iridates. *Phys. Rev. B* **83**, 205101 (2011).
35. Xu, G., Weng, H., Wang, Z., Dai, X. & Fang, Z. Chern semimetal and the quantized anomalous Hall effect in HgCr₂Se₄. *Phys. Rev. Lett.* **107**, 186806 (2011).
36. Burkov, A. A. & Balents, L. Weyl semimetal in a topological insulator multilayer. *Phys. Rev. Lett.* **107**, 127205 (2011).
37. Weng, H. M. *et al.* Weyl semimetal phase in noncentrosymmetric transition-metal monophosphides. *Phys. Rev. X* **5**, 011029 (2015).
38. Lv, B. Q. *et al.* Observation of Weyl nodes in TaAs. *Nat. Phys.* **11**, 724–727 (2015).
39. Yang, L. X. *et al.* Weyl semimetal phase in the non-centrosymmetric compound TaAs. *Nat. Phys.* **11**, 728–732 (2015).
40. Aji, V. Adler-Bell-Jackiw anomaly in Weyl semi-metals: application to pyrochlore iridates. *Phys. Rev. B* **85**, 241101 (2012).
41. Son, D. T. & Spivak, B. Z. Chiral anomaly and classical negative magnetoresistance of Weyl metals. *Phys. Rev. B* **88**, 104412 (2013).
42. Kim, H.-J. *et al.* Dirac versus Weyl fermions in topological insulators: Adler-Bell-Jackiw anomaly in transport phenomena. *Phys. Rev. Lett.* **111**, 246603 (2013).
43. Parameswaran, S. A., Grover, T., Abanin, D. A., Pesin, D. A. & Vishwanath, A. Probing the chiral anomaly with nonlocal transport in three-dimensional topological semimetals. *Phys. Rev. X* **4**, 031035 (2014).
44. Burkov, A. A. Chiral anomaly and diffusive magnetotransport in Weyl metals. *Phys. Rev. Lett.* **113**, 247203 (2014).
45. Kim, K.-S., Kim, H.-J. & Sasaki, M. Boltzmann equation approach to anomalous transport in a Weyl metal. *Phys. Rev. B* **89**, 195137 (2014).
46. Huang, X. C. *et al.* Observation of the chiral-anomaly-induced negative magnetoresistance in 3D Weyl semimetal TaAs. *Phys. Rev. X* **5**, 031023 (2015).
47. Liu, Z. K. *et al.* Discovery of a three-dimensional topological Dirac semimetal Na₃Bi. *Science* **343**, 864–867 (2014).
48. Neupane, M. *et al.* Observation of a three-dimensional topological Dirac semimetal phase in high-mobility Cd₃As₂. *Nat. Commun.* **5**, 3786 (2014).
49. Borisenko, S. *et al.* Experimental realization of a three-dimensional Dirac semimetal. *Phys. Rev. Lett.* **113**, 027603 (2014).
50. Argyres, P. N. & Adams, E. N. Longitudinal magnetoresistance in the quantum limit. *Phys. Rev.* **104**, 900–908 (1956).
51. Fauqué, B. *et al.* Two phase transitions induced by a magnetic field in graphite. *Phys. Rev. Lett.* **110**, 266601 (2013).
52. Li, Q. *et al.* Chiral magnetic effect in ZrTe₅. *Nat. Phys.* (in the press).
53. Tajima, N., Sugawara, S., Kato, R., Nishio, Y. & Kajita, K. Effects of the zero-mode Landau level on inter-layer magnetoresistance in multilayer massless Dirac fermion systems. *Phys. Rev. Lett.* **102**, 176403 (2009).

Acknowledgements

We thank S. Das Sarma, V. Yakovenko, L. Balents, E. Abrahams and J. Pixley for useful discussions. The NHMFL is supported by NSF through NSF-DMR-1157490 and the State of Florida. N.K. acknowledges the support from the overseas researcher dispatch program at NIMS. P.M.C.R. and N.E.H. acknowledge the support of the HFML-RU/FOM, member of the European Magnetic Field Laboratory (EMFL). Y.M. is supported by the MEXT KAKENHI 15H05852. L.B. is supported by DOE-BES through award DE-SC0002613.

Author contributions

N.K. performed the measurements and analysed the data. A.K., E.S.C., D.G., R.B., J.S.B., S.U., K.S., T.T., P.M.C.R. and N.E.H. contributed to the collection of experimental data at high magnetic fields. L.B. provided scientific guidance and P.G. the theoretical interpretation. H.T., S.Y. and Y.M. synthesized and characterized the single crystals. Y.I. and M.N. performed electron probe microanalysis of the measured single crystals, to confirm their high degree of purity. P.G., N.H. and L.B. wrote the manuscript with the input of all co-authors.

Additional information

Supplementary Information accompanies this paper at <http://www.nature.com/naturecommunications>

Competing financial interests: The authors declare no competing financial interests.

Reprints and permission information is available online at <http://npg.nature.com/reprintsandpermissions/>

How to cite this article: Kikugawa, N. *et al.* Interplanar coupling-dependent magnetoresistivity in high-purity layered metals. *Nat. Commun.* **7**:10903 doi: 10.1038/ncomms10903 (2016).



This work is licensed under a Creative Commons Attribution 4.0 International License. The images or other third party material in this article are included in the article's Creative Commons license, unless indicated otherwise in the credit line; if the material is not included under the Creative Commons license, users will need to obtain permission from the license holder to reproduce the material. To view a copy of this license, visit <http://creativecommons.org/licenses/by/4.0/>